EXPERIMENTAL STUDY OF INTERCONNECTIVITY AND GRAIN BOUNDARY WETNESS OF HYDROUS CARBONATITIC LIQUIDS IN MANTLE PERIDOTITE

LUCA SAMUELE CAPIZZI
Dipartimento di Scienze della Terra "Ardito Desio", Università di Milano, Via S. Botticelli 23, 20133 Milano

INTRODUCTION

Since the pioneering works of Streckeisen (1980), carbonatites are defined as intrusive and effusive igneous rocks which contain more than 50 wt.% of carbonate minerals and less than 20 wt.% of SiO_2. Migration of melts generated by partial melting of peridotite plays a crucial role in their segregation into larger masses that ascend and intrude overlying lithosphere as magmas. Liquids can migrate through rocks by hydraulic fracturing or by porous flow involving movements of the liquid along grain boundaries considering the percolation as the principal process in presence of a mixture with a large contrast in properties like solid and liquid phases. Consider a solid-liquid contact there are two types of interface at this contact: a solid-solid interface and a solid-liquid interface and each interface is associated with the interfacial energy. Liquid phase sintered composite materials exhibit solid-solid and solid-liquid interfaces. In composite materials, melt particles represent a dispersed phase, which is bounded with closed surfaces. The physical principle governing the grain scale melt distribution in partially molten rocks is the surface energy between grain and melt (Waff & Balau, 1979). For minerals with isotropic surface energies, the relative mineral-fluid interfacial energies can be described by dihedral angle θ (or wetting angle) between two grains and melt. Dihedral angle is critical to the distribution of melt in any partially molten material (Jurewicz & Jurewicz, 1986) and represents the intersection angle of two solid-fluid interfaces at the point of contact between grain boundary and liquid (Balau *et al.*, 1979; von Bargen & Waff, 1986). Interfacial energies, which depend on liquid and crystal compositions and on P-T conditions, can be readily measured by experiment. Three cases are significant: if the dihedral angle is 0 ° ($\gamma g\text{-}b > 2\gamma s\text{-}l$) the grain boundaries are completely wetted reducing area of solid-solid contact. If $0° < \theta < 60°$ solid-solid interfaces are stable, and any melt fraction should form an interconnected channel along all grain edges. When $\theta > 60°$ melt forms an isolated pocket. Melt infiltration will occur where grain-melt interfacial energy is low related to grain-grain interfacial energies. Melt might infiltrate crystals along planar surface or along triple junctions. Considering equilibrium setting, grains will be triple equiangular junction (120°) if the interfacial energies have the same value (Smith, 1964). Park & Yoon (1985) introduced the concept of a minimum-energy melt fraction in a crystal-melt system referring to a specific fluid fraction (φm) given by the sum of grain boundary energy (γgb) and solid/liquid interfacial energy (γs-l). The minimum interfacial energy depends on dihedral angle θ and volume liquid fraction. Assuming that the system is at equilibrium, and that the porosity is lower than the fraction defined by the minimum in the energy function the melt must infiltrate the rock in order to minimize the energy of the system (Watson, 1999).

Mass transport, *i.e.,* diffusion in phases such as solutions or melts, by thermal gradients and solid-solid interface is a process observed by Soret (1879) placing salt solutions in a column within a temperature gradient. He observed and demonstrated how this solution developed a concentration gradient in two components. The chemical concentration of salt migrated at the cold part of column and the lighter element toward in the hotter part. Dissolution-(re-)precipitation mechanism as a promoter of melt infiltration was invoked by Hammouda & Laporte (2000), performing experiments with dunite and Na_2CO_3 melt. This process progressed in three steps: first dunite dissolution occurred ahead of infiltration front creating new porosity and formation of interconnected melt channels allowing infiltration; secondly this dissolved material was transported by diffusion and it finally reached the carbonatite inducing olivine growth at the carbonatite-dunite contact.

Another factor promoting infiltration is the chemical gradient in partially molten system. Those fluids and therefore melts become concentrated into elongated pores parallel to the thermal gradient. This channelization is

responsible for an increase of permeability therefore affecting the transport properties of rocks at depth and that channel morphology varied with rock type. This mechanism is therefore promoted not only by thermal gradient but also by strong gradients in fluid composition, especially XCO_2, *i.e.,* gradients in concentration that, similarly to the *Soret effect*, imply gradients in chemical potential.

The goal of this work was a quantitative laboratory assessment of variables and processes controlling the ascent, mobility and connectivity of carbonatites in the mantle peridotite. The project focused on the experimental reproduction of rock textures resulting from the infiltration of hydrous carbonatitic liquids in ultramafic. We chose to investigate hydrous carbonatitic liquids at upper mantle conditions (P = 2.5 GPa and T = 1200°C) considering the system $CaCO_3$-$MgCO_3$-$FeCO_3$ as representative of natural carbonate component of carbonatitic magmas, therefore neglecting here the role of alkali.

The objectives of this research were to investigate and verify differences in dihedral angle between hydrous and anhydrous carbonatitic liquids previously studied. In addition to this, we compared the volume proportions of volatile-rich carbonatitic melts with silicate melts in partially molten peridotite, and with H_2O- or CO_2-rich fluids in peridotite and eclogite. Last, we examined whether carbonatitic liquids were always more wetting than silicate melts.

EXPERIMENTAL AND ANALITYCAL PROCEDURES

For this experimental study we chose a synthetic dunite as a model mantle representative. The starting material was prepared from single crystals of natural San Carlos forsteritic olivine with Fo_{90} for purity, clarity and lack of inclusions. These olivine crystals were crushed by using boron carbide (B_4C) and agate mortars and sieved to pass 64 μm and to keep 38 μm mesh sieves.

The choice of the melt sources depends on the required P-T conditions, and on the occurrence of olivine as the solid buffering the liquidus surface. Natural carbonatitic liquids in equilibrium with a mantle assemblage are mainly dolomitic.

We used several different mixtures of starting materials to obtain a dolomitic liquid composition. The first mixture used (Mix.1) was obtained by mass balance calculation adopting reagent grade $CaCO_3$ as starting calcium carbonate, dolomite [Ca, $Mg(CO_3)_2$] from Bazena, Ivigtut siderite [$FeCO_3$], adding brucite [$Mg(OH)_2$] as a H_2O source. The second mixture (Mix.2) was obtained by mass balance calculation considering as starting carbonates calcite, Pinerolo magnesite ($MgCO_3$) and Ivigtut siderite. As hydrous source with Mix 2, we used free water added with μL-graduate syringe (5 or 30 wt.%), or brucite + graphite powder, or brucite + quartz powder (1:1 molar) + graphite powder to balance magnesium excess due to simultaneous presence of $MgCO_3$ and $Mg(OH)_2$.

In this study a Single stage piston-cylinder apparatus was employed to reach sintering of natural San Carlos forsterite. Sintering experiments were conducted in a single different type of capsule geometry. Single molybdenum (Mo) capsule loaded with San Carlos Olivine powder in an inner graphite capsule. Sintering experiments were carried out at pressure of 0.8 GPa and temperature of 1200°C. These sintering experiments were performed for a variable run time from 30 hours to 5 days.

After the experiments the Mo capsules were cut by means diamond saw to obtain dunite cylindrical rods to be used for infiltration experiments. In this research an end-load and an end-load rocking piston-cylinder apparatuses were employed to reach high-P and high-T conditions in infiltrations experiments. Infiltration experiments were performed at P of 2.5 GPa and T of 1200°C. We carried out 19 time-resolved experiments with run times from 3 to 300 hours. After experimental runs the capsules were extract from assemblies and embedded in epoxy resin and polished by means of sandpaper and diamond paste in order to perform EDS, WDS electron microprobe analysis, X-ray maps of elements and EBSD analysis. The Electron Microprobe Analyzer (EMPA) allows us to characterize chemically the run products and to obtain information of texturally features. The EBSD analysis has been used to retrieve the misorientation of olivine grains, therefore to reconstruct grain

boundaries. EBSD output images have been also used to estimate the size of olivine crystals and of quenched carbonate products.

RESULTS

Experimental products were olivine crystals characterized by a Mg composition with a forsterite content ranging from Fo_{82} to Fo_{99}. In several experimental samples orthopyroxenes and clinopyroxenes were found. The orthopyroxene grains were Mg-rich and were classified as enstatite following the Morimoto *et al.* (1988) classification scheme; clinopyroxenes were found in a several experiments and were classified as augite and diopside. Spinel crystals were present in four experiments (found by means of Cr X-ray map) as Chromium-spinel, probably due to the presence of inclusions in natural San Carlos olivine. Periclase and ferropericlase globules or grains crystallized due to an excess of magnesium from magnesite/dolomite, or as a result of fractionation from brucite decomposition into the run charge; alternatively, it was the result of the loss of iron from olivine crystals and siderite powder mixture to capsule material. Carbonate "phases" were present in all experiments as carbonate crystals, carbonate quenched dendrites/feathers and carbonate/silicate (called carbonatite in *sensu latu* in this work) quenched intergrowths. The compositions of carbonate solid phases in equilibrium were dolomitic and magnesitic. Carbonate quenched products were present in almost all runs (except for 2 samples). In this section the quench products with SiO_2 presence < 1 wt.% were selected where the silicate fraction might be related to beam size compared to thickness of carbonate dendrite. Carbonatitic quenched intergrowths were present in eleven experiments and the average of chemical composition showed a wide range of silica content between 1 wt.% to ~ 30 wt.%, a calcium content ranging from ~ 7 to ~ 50 wt.%, and a MgO content ranging from ~ 46 to ~ 4 wt.%.

During the infiltration experiments at high temperature the polycrystalline aggregated continued to evolve by grain growth and melt distribution driven by the interfacial energy. During this stage in these infiltrations experiments some microstructure might be created by growth and by melt mobility into the charge. These microstructures called by Cmiral *et al.* (1998) *large interserts*, *triple junctions* and *layers* occurred in the experimental samples. In most cases the infiltrated melt resided in large interserts involving more than three olivine crystals (four or more) with elongated planar or rounded edges. In the experimental samples it was possible to observe different liquid distribution at different run time, bulk or geometry capsule setup. Several samples showed melt more evenly distributed over the whole charge and some areas contained the melt in separated pocket with dunite rod below carbonatitic reservoir and brucite as hydrous source, or short run experiment (3 hours duration) with 5 wt.% of free water and dunite rod above the carbonate mixture powder.

In most cases the infiltrated melts formed an interconnected channel of layers between two or more melt pockets in triple junction or in large interserts giving rise to a thrust channelization saw in a long run duration experiment (300 h) with brucite and dunite rod below carbonatitic reservoir; the run charge in this example was divided into a portion with channelization (close to dunite-carbonate interface) and a portion below with porous flow infiltration (Fig. 1). A less pronounced channelization was noted in experiments of 48 hours and with water content of 30 wt.%. The first step in the characterization of melt dihedral angles and in the measurement of melt wetting was simply to examine the sample at high resolution in BSE images combined with calcium X-ray map (Ca). Tessellation and processing of the compositional map images and measurement of the dihedral angle was performed using a customized dynamic routine developed as Mathematica® notebook. The dihedral angle measurements were carried out in six experiments with different capsule geometry, run time and bulk compositions. Considering that the two-dimensional surface of the polished mount represented a plane through a three-dimensional microstructure, the dihedral angles measured in the plane of the section did not represent true dihedral angle but the apparent dihedral angle. The true dihedral angle could be obtained from the median value on a cumulative frequency curve constructed from measurements of observed apparent dihedral angles (Hunter & McKenzie, 1989). In the longest run performed in this study the median point on the curve indicated a value of true dihedral angle of 40.8°. In the 30 hours run the median point yielded a lower value of θ of 34.15°. The

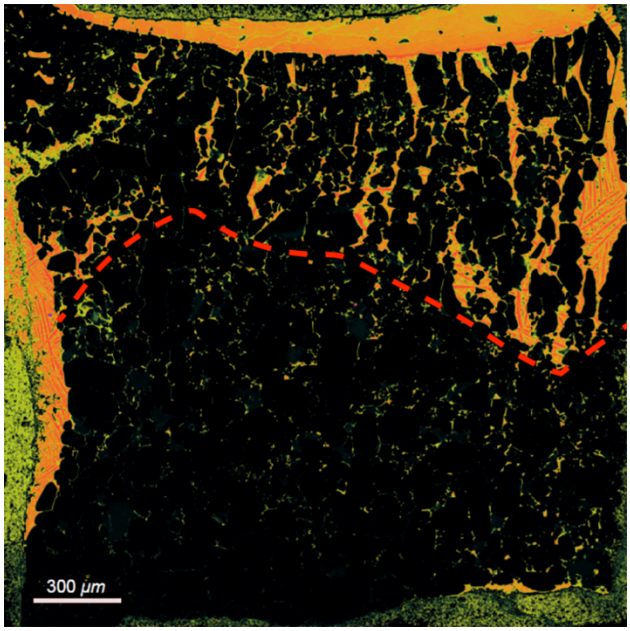

Fig. 1 - Ca X-ray map that shows how this sample could be divided into two zones. Black=Dunite rod; Orange/Yellow = carbonate melt.

two short run experiments considered here devoted to measurement of dihedral angles showed the true values of 31.5° and 32.6°, values that are strictly comparable, and that are lower than those obtained during the 30 hours run time experiment. Finally, the experiments performed with 30 wt.% of water content highlighted true dihedral angle much larger, reaching almost 50°. The dihedral angles measured showed different values. The lowest true dihedral angle values were representative of the shorter run time experiment independently from the different bulk carbonatitic reservoir composition. The geometry of melt filled pores was investigated quantitatively by measuring the grain boundary wetness, which was defined as the ratio of solid-liquid boundary area over the total area of interphase boundaries. In long run sample we performed EBSD analysis that allowed us to define clearly the olivine grain boundaries and liquid "grain" boundaries too. In order to calculate the grain boundary wetness, the EBSD output image data of olivine grain boundaries, and calcium X-ray map of carbonatitic "liquid" boundaries were combined. The EBSD olivine grain boundaries and liquids boundaries images were arbitrarily subdivided into two different images because this sample was characterized by two distinct portions where different amounts of infiltrated liquid were differently distributed as melt pockets or in interconnected channels; moreover a grain boundary wetness values of 0.144 and 0.025 were measured. The volume liquid fraction infiltrated into the peridotitic matrix was calculate by processing the Ca and Si X-ray maps, using a Mathematica® routine to enhance the distinction between melt (characterized by calcium presence) and solid. After calculations of silica and calcium percentage in each experiment we a percentage of volume liquid fraction infiltrated in the experimental sample were obtained and these values are listed in Table 1.

These results can be compared to the volume liquid fraction obtained by Hammouda & Laporte (2000) infiltrating a dunite with carbonatitic melts. These authors measured a volume of Na_2CO_3 liquid infiltrated into dunite of 18% related with a wetting angle of 30°. Overall, the values found in this work were invariably lower.

Table 1 - Calculations of percentage of volume of COH liquid infiltrated into the dunite matrix represented here by the Ca/(Ca+Si) ratio in selected runs.

Run	Ca	Si	Ca/(Ca+Si) %
LSI_4 (more infiltrated)	4.76	25.34	15.81
LSI_4 (less infiltrated)	1.08	45.04	2.35
LSI_9	9.25	79.13	10.47
LSI_10	6.05	66.07	8.39
LSI_18	6.97	73.71	8.64
LSI_19	1.77	60.99	4.00

The comparison between the portion characterized by porous flow infiltration of long run duration sample and the anhydrous samples reported in literature seems to indicate a dependence with the water presence and the run duration. In fact, the volume of hydrous carbonatitic liquid infiltrated resulted to be lower than anhydrous liquids. The 2 vol% of hydrous carbonatitic liquids infiltrated in long run duration experiment resulted to be lower than medium and short run experiments with ~ 8-10 vol%. For this reason, it seems to be a dependence between volume infiltrated melts and run duration experiments. Furthermore, the

experiments with high water content (30 wt.%) and 48 hours duration presented a volume of liquid infiltrated into the dunite between 4 to 9 vol% with higher measured (almost 50°) wetting angles.

DISCUSSION

Variability of wetting angle

The behaviour of carbonate melts was previously investigated and the experimental characterizations considering dihedral angle of liquids infiltrated in a peridotitic matrix with their results are listed in Table 2.

Table 2 - Previous experimental dihedral angle measured in literature between peridotitic matrix and carbonatitic reservoir.

	Capsule material	Run Time (h)	Starting Material	θ measured (°)	Pressure (Gpa)	Temperature (°C)
Hunter and McKenzie (1989)	Pt	92	sp-lherz + $MgCa(CO_3)_2$	28	3	1290
Watson et al. (1990)	Pt	24 - 144	S.C.ol + Na_2CO_3 S.C.ol + K_2CO_3 S.C.ol + $CaCO_3$+H_2O	23 - 26	1-3	1300
Minarik and Watson (1995)	Ti+grph	10 - 20	S.C.ol + Na_2CO_3	25 - 30	1	1300
Hammouda and Laporte (2000)	Pt	0.16 - 95	S.C.ol(+MgO-SiO_2) + Na_2CO_3	30	1	1300

From the wetting angle measurements, we can state that the true θ values for hydrous carbonatitic liquids are higher compared to anhydrous wetting angles reported in literature (Table. 2). These differences may be due to the bulk carbonate compositions, but also to the experimental run durations. Possibly, the most crucial factor is the presence and amount of water in the experimental setup, as seen this work. The description of dihedral angle as a key parameter to interpret the behaviour of liquids in solid matrix (mantle or crustal lithologies) is of primary concern not only in systems involving carbonate or carbonatitic melts, but obviously also using silicate melts as liquid fraction. The dihedral angle values in a silicatic system reported measure of θ from 50° to 10° considering the differences in temperature (from 1360°C to 1200°C) and pressure (1-3 GPa); moreover it is evident the crucial importance of the image resolution on which angles were measured which are smaller in comparison to this work (Waff & Balau, 1979; Toramaru & Fujii, 1986; Daines & Kohlstedt, 1993; Cmiral *et al.*, 1998; Yoshino *et al.*, 2005; Faul & Scott, 2006; Yoshino *et al.*, 2009).

The evolution of pore geometry, channelization and Grain boundary wetness

Liquid-phase sintering (LPS) is a process for forming multiphase dense materials from powder aggregates. LSP involve the sintering process where liquid and solid phases coexist (German *et al.*, 2009). In LPS case involving both liquids and vapours again with solid phase, the solid-vapour dihedral angle is at the intersection between grains and vapour phases but where liquid phase is involved the angle is within the intersection of the grains contacts with liquid phase. Microstructures are constantly evolving with time during the sintering process and the final structure (with prolonged sintering) evolves until a single grain, or crystal, configuration with a structure well developed by time and small changes at the solid-liquid surface energy are able to give liquid penetration of grain boundary. In the first step of sintering the dihedral angles and the whole system tends to the equilibrium condition with a decrease in wetting angle values with time. In the late stage of densification, grain boundary development and annealing processes move the interfaces toward equilibrium, with a progressive growth of sintering necks, migration of grain boundaries and reduction of interstitial liquid fraction.

The experiments of this work, representative of a wetting liquid, can be interpreted in this theoretical frame with an increase of θ due to a sintering process, since after liquid formation the low dihedral angles enable liquid penetration; therefore the solid-liquid system and the evolution of wetting angle tend to equilibrium condition as a function of time (Fig. 2). The experimental results evidenced the channelization of pores due to

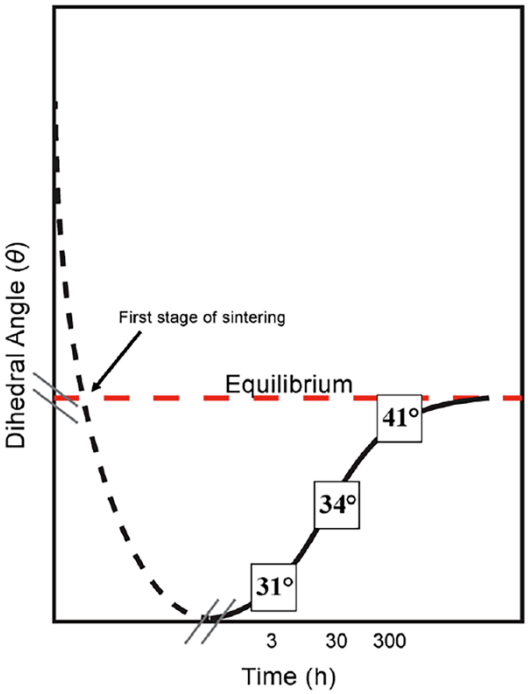

Fig. 2 - Schematic diagram showing the relationships between dihedral angle values with time. The first stage of sintering, not occurring in the experiments, highlights a decrease of wetting angle values with time (ramp down), whereas in the ramp up it is possible to observe an increasing of wetting angle with run time experiment underlined by the measured true dihedral angle values (modified from German *et al.*, 2009).

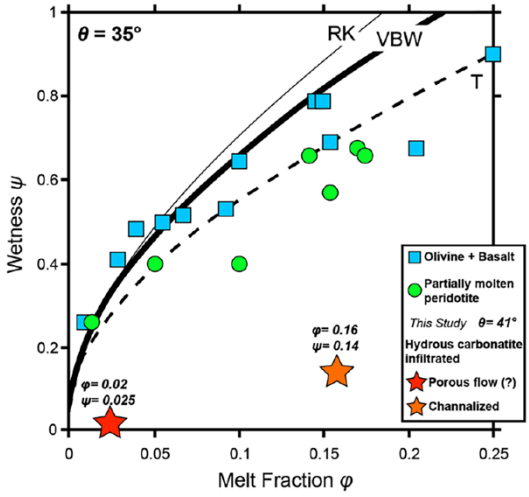

Fig. 3 - Plot of wetness and melt fraction related of olivine + basalt and partially molten peridotite systems from Yoshino *et al.* (2005) compared to the experimental measured values.

gradients in temperature or chemical composition of intergranular fluid or melt at lithospheric mantle conditions. In the long time experiment two different infiltrated melt behaviour from top to bottom of the run charge were observed and the run charge was interpreted with interconnected channels as a result of channelization. Channelization is highlighted when grain boundary wetness is compared to the fraction of liquid infiltrated in the solid matrix. Therefore the volume liquid fractions infiltrated into the dunite rod (measured for the two different parts of the sample) were compared with the calculated grain boundary wetness in this sample comparing with grain boundary wetness measured by Yoshino *et al.* (2005).

The low grain boundary wetness the experiment performed in this work may be due to relatively low liquid-solid interfaces which develop if the liquid is channelized and the portion with melt pocket is not representative of porous flow infiltration; nevertheless it should be also related to a channelization processes possibly evolving to channelization with time (Fig. 3).

A reversal in the wettability of carbonatitic vs. silicate magma

In order to assess the wetting angle variation between olivine matrix and a MORB melt, Yoshino *et al.* (2009) fitted the experimental data through parabolic equation. Then they calculated the melt composition in equilibrium with olivine and constructed a contour map of wetting angle for different temperatures and pressures. Their results illustrate the dependence of dihedral angle on melt structure in partially molten peridotite and demonstrate that temperature is the most important variable in controlling variations of dihedral angle. As the solidus for carbonatitic magmas is located at relatively low temperature, it is therefore a common assumption that carbonatitic liquids are more wetting than basaltic melts, and therefore more mobile. Nonetheless, water is believed to be an important component of carbonatitic liquids and it plays a crucial role in many carbonatite magma models. It was assumed that the water solubility in the carbonate melts was in the order of 14 wt.% at low pressure and relatively high temperature (0.225 GPa and 900°C; Keppler, 2003) and 10 wt.% at even lower pressure of 0.1 GPa and temperature between 700°C to 900°C (Veksler & Keppler, 2000), which is two to three times higher than the value observed for most silicate liquids under same or

similar pressure and temperature conditions (Behrens, 1995). For these reasons, we can assume that water partitions preferably into carbonatitic melts compared to silicate melts at similar P-T conditions.

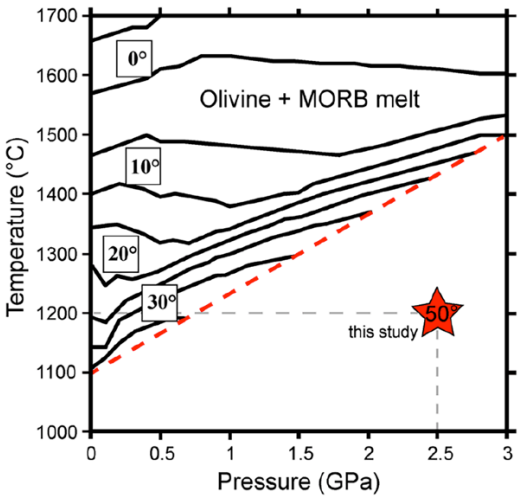

Fig. 4 - Isopleths diagram of the dihedral angles values in olivine - MORB liquid system for the model mantle compositions in P-T space. Dashed red line represents the solidus curve in the peridotite system from Herzberg *et al.* (2000). Red star represents the P-T conditions of the experiments performed with 30 wt.% of water content with true dihedral angle measured of ~ 50°.

The comparison between the true wetting angle measured for the experimental runs at high water content (experiments with 30 wt.% of water at P = 2.5 GPa and T = 1200°C) and the olivine + MORB melt systems studied by Yoshino *et al.* (2009) showed how the wetting angles of silicate melts have much lower values than those of carbonatitic liquids which are unexpectedly high.

The Fig. 4 shows the dependence of wetting angle on melt structure and composition which tend to be smaller in a system where the liquid phase has a similar composition with the solid phase (MORB + olivine), considering that melt structure is related by the degree of polymerization. Considering the inability to polymerize to form network structures of carbonate ions and the presence of water in the system, which involve hydroxyl bonds highlighting negative effect on stability structures and polymerization, the experimental results of this work can be also explained in this frame.

CONCLUSIONS

Knowledge of pore geometry is essential to understanding bulk physical properties, interconnectivity and mobility mechanisms of melts in partially molten rocks.

The equilibrium of pore geometry can be determined by knowing the porosity and the dihedral angle, which is determined by the ratio of solid-solid and solid-liquid interfacial energies. Measurements of the dihedral angle has been the most common way to assess the geometry and connectivity of intergranular liquids by researchers that have investigated the dihedral angles of the geometry of anhydrous carbonatitic melts, C-O-H fluids and silicate melts in various silicate mineral aggregates at various pressure and temperature conditions.

The experimental results of this work in the hydrous carbonatitic liquids in the dunite matrix system suggested several differences between the system of this work and silicate or anhydrous carbonatitic melts in different silicate aggregates in terms of dihedral angle values and grain boundary wetness. The variability of wetting angle suggested that the addition of water into a carbonatitic melt solution compared with silicate and anhydrous carbonatitic melts, or compared with volatile rich fluids, shifted the dihedral angle toward values significantly higher than 30°, up to 48-50° for liquids with high dissolved H_2O.

Considering that the evolution of pore geometry changes with time it has been demonstrated that the experiments of this work could be represented in this frame presenting similar behavior. Different stages of channelization of pores filled by hydrous carbonatitic liquid due to gradient of temperature and chemical composition were demonstrated. Moreover, different infiltration behaviors underlined comparing the grain boundary wetness with volume liquid infiltrated into the dunite rod were noted. This difference was interpreted as due to a channelization process evolving from “microchannelization” of pore with time.

Although it is widely assumed that carbonatitic liquids are more wetting and more mobile than silicate magmas, if H_2O is available, H_2O partitions into carbonatitic liquids rather than in silicate liquids at the same P-T conditions should be expected. The dihedral angle measured in this work may evolve up to 50°, a value higher than that silicate melts at similar mantle conditions. If silicate and carbonatitic liquids maintain

immiscibility, water-rich carbonatitic liquid may segregate and conserve their identity in an olivine mantle solid matrix.

REFERENCES

Balau, J.R., Waff, H.S., Tyburczy, J.A. (1979): Mechanical and thermodynamic constraints on fluid distribution in partial melts. *J. Geophys. Res*., **84**, 6102-6108.

Behrens, H. (1995) Determinations of water solubilities in high - viscosity melts: An experimental study on $NaAlSi_3O_8$ melts. *Eur. J. Mineral.*, **7**, 905-920.

Cmiral, M., Fitz Gerald, J.D., Faul, U.H., Green, D.H. (1998): A close look at dihedral angles and melt geometry in olivine - basalt aggregates: a TEM study. *Contrib. Mineral. Petr.*, **130**, 336-345.

Daines, M.J. & Kohlstedt, D.L. (1993): A laboratory study of melt migration. *Philo. T. R. Soc. London*, **342**, 43-52.

Faul, U.H. & Scott, D. (2006): Grain growth in partially molten olivine aggregates. *Contrib. Mineral. Petr.*, **151**, 101-111.

German, R.M., Suri, P., Park, S.J. (2009): Review: liquid phase sintering. *J. Mater. Sci.*, **44**, 1-39.

Hammouda, T. & Laporte, D. (2000): Ultrafast mantle impregnation by carbonatite melts. *Geology*, **28(3)**, 283-285.

Hunter, R.H. & McKenzie, D. (1989): The equilibrium geometry of carbonate melt in rocks of mantle composition. *Earth Planet. Sc. Lett.*, **92**, 347-356.

Jurewicz, S.R. & Jurewicz, A.J.G. (1986): Distribution of Apparent Angles on Random Sections with Emphasis on Dihedral Angle Measurements. *J. Geophys. Res.*, **91**, 9277-9282.

Keppler, H. (2003): Water solubility in carbonatite melts. *Am. Mineral.*, **88**, 1822-1824.

Minarik, W.G. & Watson, E.B. (1995): Interconnectivity of carbonate melt at low melt fraction. *Earth Planet. Sc. Lett.*, **133**, 423-437.

Morimoto, N., Fabries, J., Ferguson, A.K., Ginzburg, I.V., Ross, M., Seifert, F.A., Zussman, J., Aoki, K., Gottardi, G. (1988): Nomenclature of clinopyroxenes. *Am. Mineral.*, **73**, 1123-1133.

Park, H.H. & Yoon, D.N. (1985): Effect of Dihedral Angle on the morphology of grains in a matrix phase. *Metall. Trans. A*, **16A**, 923-928.

Smith, C.S. (1964): Some elementary principles of polycrystalline microstructure. *Metall. Rev.*, **9**, 1-47.

Soret, C. (1879): Sur l'ètat d'èquilibre que prend au point de vue de sa concentration une dissolution saline primitivement homogène dont deux parties sont portèes à des temperatures differentes. *Arch. Geneve*, **2**, 48-61.

Streckeisen, A. (1980): Classification and nomenclature of volcanic rocks, lamprophyres, carbonatites and melilitic rocks. IUGS Subcommission on the systematics of Igneous Rocks. *Geol. Rundsc.*, **69**, 194-207.

Toramaru, A. & Fujii, N. (1986): Connectivity of melt phase in a partially molten peridotite. *J. Geophys. Res.*, 91, 9239-9252.

Veksler, I.V. & Keppler, H. (2000): Partitioning of Mg, Ca, and Na between carbonatite melt and hydrous fluid at 0.1 - 0.2 GPa. *Contrib. Mineral. Petr.*, **138**, 27-34.

von Bargen, N. & Waff, H.S. (1986): Permeabilities, interfacial areas and curvatures of partially molten system: results of numerical computations of equilibrium microstructures. *J. Geophys. Res.*, **91**, 9261-9276.

Waff, H.S. & Balau, J.R. (1979): Equilibrium fluid distribution in an ultramafic melt under hydrostatic stress conditions. *J. Geophys. Res.*, **84**, 6109-6114.

Watson, E.B. (1999): Lithologic partitioning of fluids and melts. *Am. Mineral.*, **84**, 1693-1710.

Yoshino, T., Takei, Y., Wark, D.A., Watson, E.B. (2005): Grain boundary wetness of texturally equilibrated rocks, with implications for seismic properties of the upper mantle. *J. Geophys. Res.*, **110**, B08205. doi:10.1029/2004JB003544.

Yoshino, T., Yamazaki, D., Mibe, K. (2009:) Well-wetted olivine grain boundaries in partially molten peridotite in the asthenosphere. *Earth Planet. Sc. Lett.*, **283**, 167-173.